Human crossfeed in dual-axis manual control with motion feedback

Barendswaard, Sarah; Pool, Daan; Mulder, Max

Important note
To cite this publication, please use the final published version (if applicable).
Please check the document version above.

Human Crossfeed in Dual-Axis Manual Control with Motion Feedback

S. Barendswaard, D.M. Pool and M. Mulder [*]

[*] *Control and Simulation Section, Aerospace Engineering, Delft University of Technology, 2629 HS, Delft, The Netherlands (e-mail: {s.barendswaard, d.m.pool, m.mulder}@tudelft.nl).*

Abstract: While many realistic manual control tasks require human operators to control multiple degrees-of-freedom simultaneously, our understanding of such multi-axis manual control has not moved far beyond considering it simply as the control of multiple fully-independent axes. This investigation aims to further our understanding of multi-axis control by focusing on one phenomenon that is known to occur in such tasks: crossfeed. Crossfeed occurs when operators' inputs in one controlled axis feed into another controlled degree-of-freedom, thereby affecting overall control performance. A human-in-the-loop experiment, in which operators performed a dual-axis aircraft roll and pitch tracking task with physical motion feedback, was conducted in the SIMONA Research Simulator at TU Delft. Three conditions were tested: the full dual-axis control task, supplemented with reference single-axis roll and pitch tasks. Through the use of independent target and disturbance forcing function signals in both controlled axes, we were able to detect the presence of crossfeed in this dual-axis task from spectral analysis. Furthermore, these signals facilitated the objective identification of the dynamics of the crossfeed contribution, in parallel with estimating operators visual and motion responses. The crossfeed dynamics were found to resemble the well-known dynamics of human operators' visual responses. The crossfeed contribution was found to explain up to 20% of the measured control inputs, thereby indicating that crossfeed can be a factor of significance in multi-axis manual control.

Keywords: manual control, multi-axis control, human operator modeling, crossfeed

1. INTRODUCTION

Despite the fact that most operationally relevant manual control tasks – especially those in the aerospace domain – typically require human operators to perform simultaneous control of multiple degrees-of-freedom, our understanding of the intricacies of such multi-axis control is still severely limited. In fact, the current state-of-the-art for the analysis and modeling of multi-axis manual control is to simply account for multiple *independent* single-axis tasks (Stapleford et al., 1967; Zaal and Pool, 2014; Hess, 2015). While somewhat successful, such approaches cannot account for the inherently multi-input-multi-output nature of the human operator in a multi-axis case, where due to task and operator limitations couplings between operators' control in different axes are likely to be present. We argue that for meaningful understanding and prediction of human operator performance in multi-axis tasks, the presence of such couplings needs to be verified, if not explicitly accounted for in our analysis methods and operator models.

Early investigations into human control in dual-axis tasks have shown that marked differences with single-axis manual control do indeed exist (Bekey et al., 1965; Todosiev, 1967; Levison et al., 1971; Van Lunteren, 1979). For instance, degraded task performance has been reported in dual-axis tracking, in addition to increased operator remnant levels. While some studies have postulated that this may be explained by a systematic reduction in operator aggressiveness (reduced crossover frequency) compared to the single-axis case (Bergeron et al., 1971; Hess, 2015), others have proposed that the characterization of multi-axis control should include task interference phenomena, such as those resulting from divided attention (e.g., switching between axes) and cross-couplings between the different controlled degrees-of-freedom. A number of earlier investigations (Bekey et al., 1965; Todosiev, 1967; Van Lunteren, 1979), have proposed to analyze and model *crossfeed* between axes, which occurs when operators are unable to fully decouple their separate tasks, as an additional human operator response. However, no study to date has successfully used objective human operator identification techniques to verify the presence and dynamics of such hypothesized crossfeed responses.

This investigation uses novel means to analyze the occurrence and nature of crossfeed in manual control. A human-in-the-loop experiment is performed in the SIMONA Research Simulator at TU Delft, to collect measurements of human operators in a dual-axis roll and pitch tracking task with physical motion feedback. Application of two independent multisine forcing functions in each controlled axis facilitates the *detection* of crossfeed through analysis of measured signals with spectral methods (Jex et al., 1978). Furthermore, the multi-channel human operator identification method developed by Van Paassen and Mulder (1998) is extended to facilitate the *identification* of the dynamics of the additional crossfeed responses. To verify whether the measured crossfeed may have a motoric origin
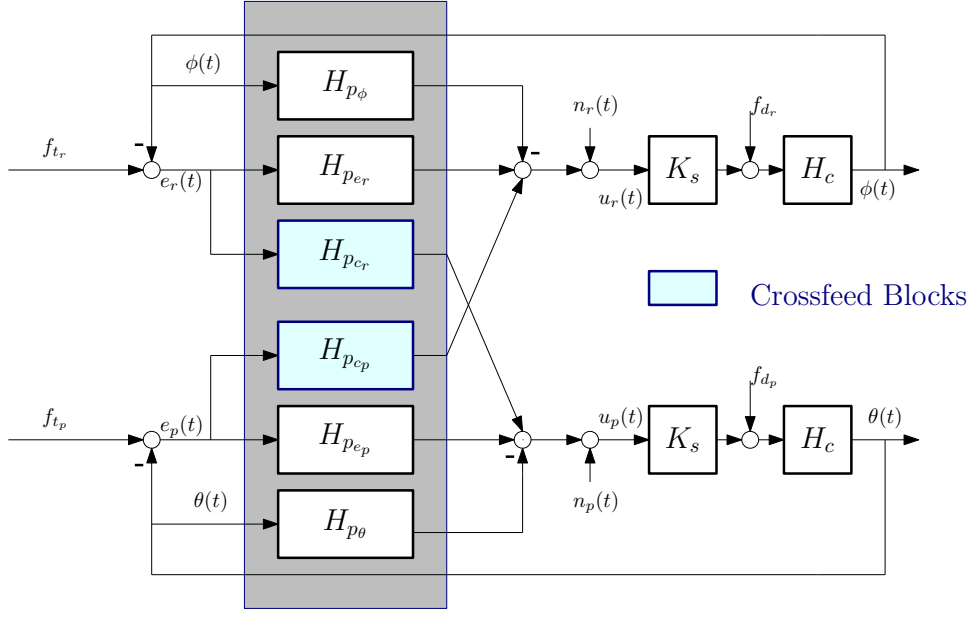
Fig. 1. Schematic representation of a dual-axis tracking task with motion feedback and crossfeed.

– i.e., due to restrictions in the movement of the operator's arm, measured single-axis task measurements are used as well as model based analysis allowed by the systems input-output signals.

This paper has the following structure. The dual-axis control task and the system identification approach for identification of human crossfeed dynamics is elaborated in Section 2. The details of the experiment and its results are presented in Sections 3 and 4, respectively. The paper ends with a discussion and conclusions.

2. CROSSFEED IDENTIFICATION APPROACH

Figure 1 shows a schematic representation of a dual-axis tracking task with motion feedback, where possible crossfeed between the controlled roll (ϕ) and pitch (θ) axes is explicitly accounted for. In this representation, the operator controls the system based on feedback of the (visually presented) tracking errors – e_r and e_θ for roll and pitch, respectively – as well as physical motion feedback of the controlled system's roll and pitch attitudes. Finally, crossfeed is accounted for with additional responses – indicated with transfer blocks $H_{p_{c_r}}$ and $H_{p_{c_p}}$, that transfer the tracking error in one axis to the operator control input u in the other axis. For the roll axis, the following expression may thus be derived for the total human operator control input u_r from Figure 1:

$$U_r(j\omega) = E_r(j\omega)H_{p_{e_r}}(j\omega) + E_p(j\omega)H_{p_{c_p}}(j\omega) + \Phi(j\omega)H_{p_\phi}(j\omega) + N_r(j\omega) \quad (1)$$

An equation similar to Eq. (1) can also be derived for the pitch axis control input u_p.

For identification of the human operator, we would have to solve Eq. (1) for its three unknowns: $H_{p_{e_r}}(j\omega)$, $H_{p_{c_p}}(j\omega)$ and $H_{p_\phi}(j\omega)$. To achieve this, we have extended the

objective human operator identification method developed by Van Paassen and Mulder (1998). This method is a frequency-domain identification technique that can be used without any prior knowledge about the dynamics of the system to be identified. Van Paassen and Mulder (1998)'s method uses *two* independent multisine target and disturbance forcing function signals (e.g., f_{t_r} and f_{d_r} in Figure 1) to identify *two* human operator responses ($H_{p_{e_r}}$ and H_{p_ϕ} in Figure 1) in a single-axis task, by interpolating between the frequencies excited by both applied forcing function signals. For the dual-axis task of Figure 1, we have derived a similar method, where for identification of the additional unknown crossfeed response $H_{p_{c_p}}$, we use additional independent forcing function components *from the other axis*. To be successful, this requires that all four forcing function signals shown in Figure 1 be independent, i.e., be composed for sines with different frequencies.

If this requirement is met, following the same procedure as proposed by Van Paassen and Mulder (1998), the following system of three equations may be derived by evaluating Eq. (1) at each of the frequencies of f_{t_r}, as well as by interpolating from the frequencies of f_{d_r} and f_{t_p}, as indicated by the superscripted symbols:

$$\begin{pmatrix} U_r^{t_r} \\ \tilde{U}_r^{d_r} \\ \tilde{U}_r^{t_p} \end{pmatrix} = \begin{pmatrix} E_r^{t_r} & E_p^{t_r} & \Phi^{t_r} \\ \tilde{E}_r^{d_r} & \tilde{E}_p^{d_r} & \tilde{\Phi}^{d_r} \\ \tilde{E}_r^{t_p} & \tilde{E}_p^{t_p} & \tilde{\Phi}^{t_p} \end{pmatrix} \begin{pmatrix} H_{p_{e_r}} \\ H_{p_{c_p}} \\ H_{p_\phi} \end{pmatrix} \quad (2)$$

Note that all variables in Eq. (2) are a function of the roll target forcing function frequency ($j\omega_{t_r}$), even though this indication is dropped for notation purposes. The system of equations of Eq. (2) can be solved for $H_{p_{e_r}}(j\omega_{t_r})$, $H_{p_{c_p}}(j\omega_{t_r})$ and $H_{p_\phi}(j\omega_{t_r})$ from inversion of the matrix-vector equation. Furthermore, equivalent frequency response estimates can be obtained at the frequencies of f_{d_r}.

To verify the developed method described in this section, human operator simulation data was generated for the dual-axis system of Figure 1. The simulation was driven by the set of forcing functions also used for the experiment (see Section 3) and the remnant (n_r and n_p) was omitted. The results of our identification method, as shown in Fig. 2, matches well with the original specified human operator model transfer functions, thereby indicating the efficacy of the proposed method.
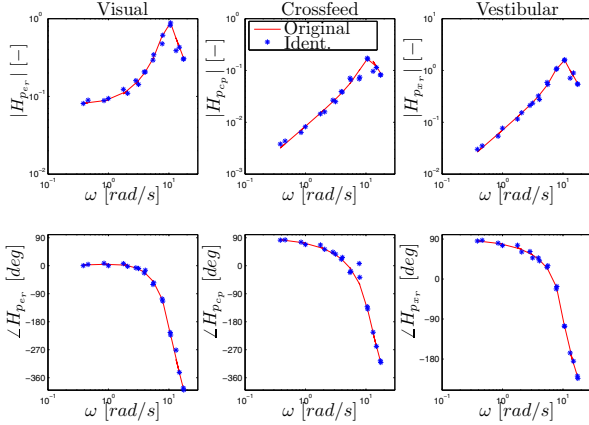

Fig. 2. Identified human operator frequency response estimates compared to original simulation model settings.

3. EXPERIMENT

To investigate the presence and dynamics of crossfeed in dual-axis manual control, an experiment was performed at the SIMONA Research Simulator (SRS) at TU Delft, see Fig. 3.

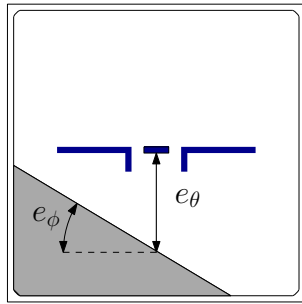
Fig. 3. The SIMONA Research Simulator.

Fig. 4. Dual-axis compensatory visual display.

3.1 Control Task

In the experiment, participants performed the dual-axis target-tracking and disturbance-rejection task depicted in Figure 1. The roll and pitch axis tracking errors – e_ϕ and e_θ, respectively – were presented on a compensatory visual display, as illustrated in Figure 4. This display, resembling a simplified artificial horizon display, shows both the roll and pitch errors. It was the participants' task to continuously minimize these tracking errors. Physical roll and pitch motion feedback, presented without any

scaling or filtering, was provided using SIMONA's motion system. Due to the motion limitations of SIMONA, the specific forces, could not be compensated for and therefore, were experienced by the subjects.

An electric sidestick was used to give roll and pitch control inputs (u_r and u_p) to the uncoupled controlled element dynamics. The controlled element dynamics were set equal for both axes, to allow for a straightforward comparison between axes. Note that in aircraft, the controlled roll and pitch dynamics are generally distinctly different. In our experiment, the controlled element dynamics were selected to be an approximation of typical aircraft attitude dynamics: a second-order system, with a break frequency at 3 rad/s, as given in Eq. (3):

$$H_c = \frac{67.9}{s(s+3)} \tag{3}$$

Note that the system defined by Eq. 3 is at a transition between single integrator dynamics K/s and double integrator K/s^2 at the frequency 3 rad/s. Therefore, this controlled element requires human operators to generate lead, which causes them to use physical motion feedback, when available (Stapleford et al., 1967; Jex et al., 1978; Pool et al., 2010). Each experiment run lasted 90 seconds, of which the final 81.92 seconds were used for data analysis.

3.2 Independent Variables

To detect and identify possible crossfeed in human operators, testing one experiment condition, namely the full dual-axis task of Fig. 1, would be sufficient. However, to facilitate direct comparison to single-axis control, as well as for investigating the origin of crossfeed, it is highly useful to also collect data for the corresponding single-axis tasks. For this reason, three conditions were in fact tested: the full dual-axis control task, supplemented with single-axis roll and pitch tasks in which the non-active axis was simply locked at 0 deg. However, the side stick was left unlocked. This was to test for motoric sources of crossfeed.

3.3 Forcing Functions

The target and disturbance forcing functions in both axes were quasi-random multisine signals, as defined by:

$$f_{d,t}(t) = \sum_{k=1}^{N_{d,t}} A_{d,t}[k] sin(\omega_{d,t}[k]t + \phi_{d,t}[k]) \tag{4}$$

Each kth sinusoid in all forcing functions is defined by its excitation frequency $\omega_{d,t}[k]$, amplitude $A_{d,t}[k]$, and phase $\phi_{d,t}[k]$. All signals are a sum of 10 sinusoids, spanning frequencies between 0.1 and 20 rad/s. The amplitude distribution of all forcing functions is defined using the low-pass filter also used by Zaal and Pool (2014). This was done to obtain low-pass signals that resemble turbulence. The numerical values of all roll and pitch forcing function data are listed in Tables 1 and 2, respectively.

3.4 Participants and Experimental Procedures

Twelve participants performed the experiment. Half of the invited participants were trained pilots, whereas the other
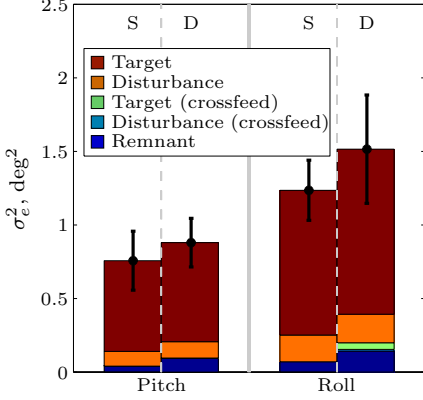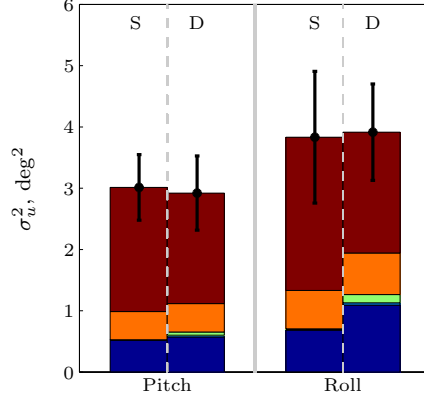
Fig. 5. Tracking error variance decomposition.

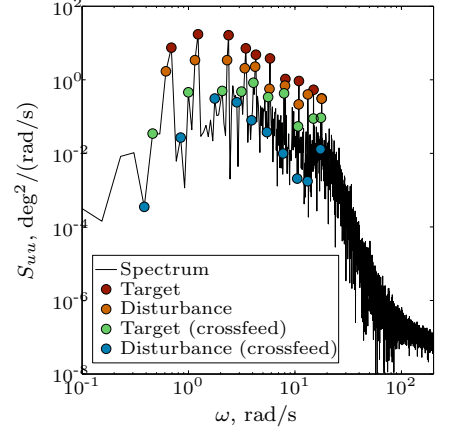Fig. 6. Control signal variance decomposition.

Fig. 7. Example PSD of $u_r(t)$ (Subject 1, dual axis).

Table 1. Roll-axis forcing function data.

disturbance, f_{d_r}				target, f_{t_r}			
n_d, –	ω_d, rad/s	A_d, deg	$\phi_{d\phi}$, rad	n_t, –	ω_t, rad/s	A_t, deg	$\phi_{t\phi}$, rad
5	0.384	0.014	1.866	6	0.460	1.657	3.489
11	0.844	0.023	5.013	13	0.997	1.159	0.656
23	1.764	0.027	2.245	27	2.071	0.523	6.169
37	2.838	0.026	3.957	41	3.145	0.282	4.723
51	3.912	0.026	3.538	53	4.065	0.189	0.405
71	5.446	0.028	7.853	73	5.599	0.117	6.201
101	7.747	0.034	5.448	103	7.900	0.074	2.662
137	10.508	0.043	4.108	139	10.661	0.054	0.183
171	13.116	0.055	7.997	194	14.880	0.042	0.607
226	17.334	0.081	6.923	229	17.564	0.039	2.072

Table 2. Pitch-axis forcing function data.

disturbance, f_{d_p}				target, f_{t_p}			
n_d, –	ω_d, rad/s	A_d, deg	$\phi_{d\phi}$, rad	n_t, –	ω_t, rad/s	A_t, deg	$\phi_{t\phi}$, rad
8	0.614	0.023	3.393	9	0.690	1.681	3.075
15	1.150	0.031	8.851	16	1.227	1.129	5.049
30	2.301	0.032	8.318	31	2.378	0.499	0.760
44	3.375	0.031	8.881	45	3.451	0.283	3.956
55	4.218	0.032	5.259	56	4.295	0.202	3.475
75	5.752	0.034	5.281	76	5.829	0.129	5.546
105	8.053	0.041	5.005	106	8.130	0.084	6.222
141	10.815	0.053	7.486	142	10.891	0.062	0.217
172	13.192	0.066	7.891	195	14.956	0.049	2.639
232	17.794	0.100	3.837	233	17.871	0.045	2.373

half were skilled non-pilots, with extensive experience from earlier experiments. Participants performed a minimum of 4-5 training runs, to allow their performance to stabilize. Thereafter, 5 more runs were collected as the measurement data. Participants were instructed to minimize the roll and pitch tracking errors. After each run, the participants were notified of their performance (RMS of the tracking errors), to motivate them to consistently perform at their best.

3.5 Dependent Variables

To compare the level task performance between single and dual-axis tracking, the variance of the roll and pitch error signals (σ_e^2) was calculated. Calculation of this variance from spectral analysis of the measured signals (Jex et al., 1978), allows for separating the individual contributions of the target and disturbance signals, as well those attributable from the target and disturbance signals from the other axis, as all provide power at independent frequencies. Similarly, the control variance (σ_u^2) is used to quantify differences in control activity between single and dual-axis tasks. Any significant variance components attributable to the off-axis' forcing functions would provide evidence for the presence of crossfeed. To analyze the crossfeed dynamics, the identification approach elaborated in Section 2 was applied to obtain frequency response estimates of human operators' visual, motion, and crossfeed responses. To quantify the practical significance of the modelled crossfeed, the modelled output contributions of the visual, vestibular and crossfeed responses are analyzed and compared. This is done with the parametric models of the three operator response functions. The individual output contribution variances are divided by the total contribution to find the percentage contribution of the separate operator responses.

4. RESULTS

4.1 Spectral Analysis of Variances

Figs. 5 and 6 show the average roll and pitch axis error and control signal variances, decomposed in components attributable to the target and disturbance forcing functions of both axes – that is, contributions from the signals of the principle axis, as well as off-axis signal contributions – and human operator remnant. Variances are shown for pitch and roll control separately. Furthermore, the left bar of each set of two corresponds to the single-axis task ("S"), while the right data is from the dual-axis task ("D").

Fig. 5 shows that, in general, tracking performance was consistently worse for roll tracking and also consistently degraded in the dual-axis task. The increased σ_e^2 for the dual-axis case is attributable to two components: an increase in the remnant contribution, as well as an added crossfeed contribution, most clearly visible in roll (light green and light blue data). Similarly, Fig. 6 also shows distinct contributions of the off-axis target and disturbance signals in the dual-axis data for the control variance. The presence of these off-axis forcing function contributions is clear evidence of the presence of crossfeed between the roll and pitch tasks. This is further confirmed from Fig. 7, which shows an example power spectral density of the roll-axis control signal u_r. The pronounced peaks at the frequencies of especially the pitch target forcing function (light green markers) in this roll-axis control spectrum are clear sign of crossfeed between both axes.
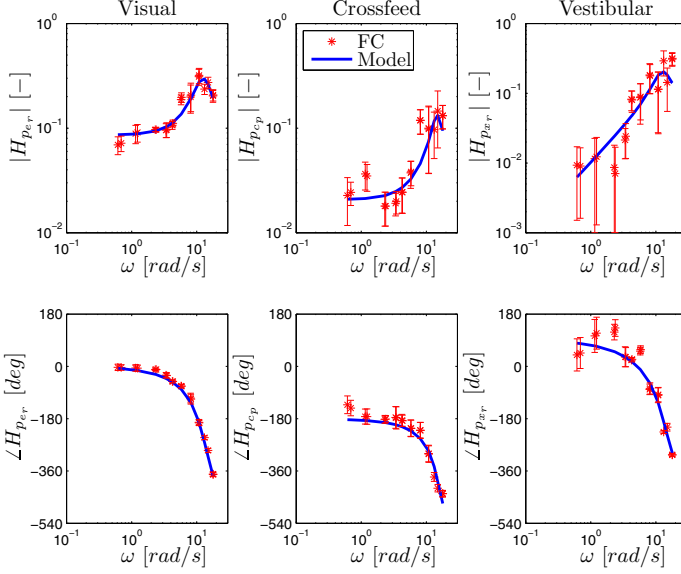
Fig. 8. Roll-axis human operator frequency response estimates (Subject 1, dual-axis task).

4.2 Operator Describing Function

Using the identification method described in Section 2, the frequency responses of the operator visual, vestibular, and crossfeed responses were estimated. Fig. 8 shows an example result, for the roll-axis human operator responses identified for Subject 1. The red stars present the identified frequency response, with the errorbars showing the 95% confidence intervals over the five measurement runs.

Fig. 8 shows consistent estimation of the dynamics of all three responses. Furthermore, in partial confirmation of earlier results (Van Lunteren, 1979; Todosiev, 1967), the dynamics of the crossfeed response appear highly similar to those of the visual response, however, with a lower gain and a 180 deg phase shift. Based on these observations, a candidate model structure for the crossfeed response, to complement well-known models for the visual and vestibular responses (Stapleford et al., 1967; Pool et al., 2010), would be identical to the widely accepted visual response model, as given by Eq. (5):

$$H_{p_{c_p}} = \frac{K_{cp}(1 + T_{L_{cp}}s)\omega_{nm_{cp}}^2}{\omega_{nm_{cp}}^2 + 2\zeta_{nm_{cp}}\omega_{nm_{cp}}s + s^2}e^{-s\tau_{cp}} \qquad (5)$$

Fig. 8 shows the fit of this model as a solid blue line. The model is seen to be able to explain the crossfeed frequency response at high accuracy. This result can be interpreted by considering the polar plots of operator's control inputs in the single-axis tracking conditions, shown in Fig. 9.

Fig. 9(a) shows that Subject 1's single-axis pitch control inputs were not perfectly aligned with the sidestick's natural pitch axis, implying that for every pitch input, a coupled crossfeed input in roll was given. Fig. 9(b) shows that this participant showed a similar, yet reduced, crossfeed from roll to pitch. The orientation of the fitted linear regression for the pitch task confirms that for a positive u_p, a negative u_r was given. This is highly consistent with the 180 deg phase shift observed for the
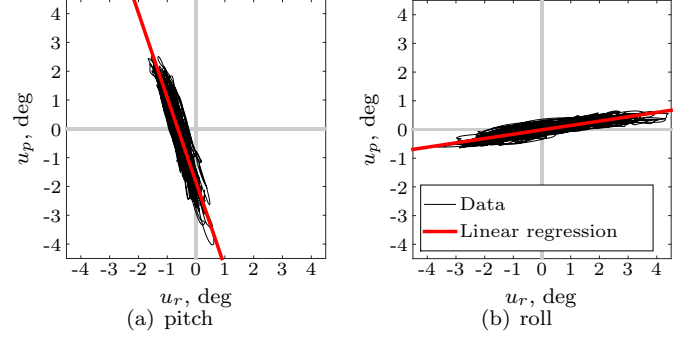

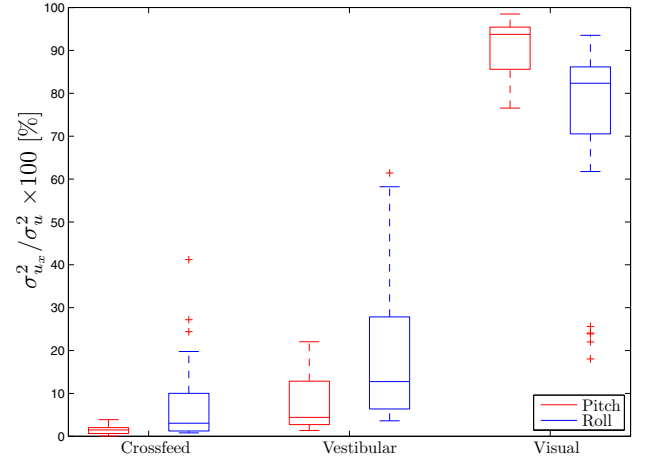Fig. 9. Single-axis control input polar plots (Subject 1).

Fig. 10. Fractions of control input variance explained by modeled visual, vestibular, and crossfeed responses.

crossfeed response in Fig. 8. This result suggests that the measured crossfeed has a strong *motoric* contribution: participants are unable to fully decouple the pitch and roll-axis tasks at the manipulator level due to the hand geometry.

Finally, from preliminary full human operator model fits, the percentage of the total modeled control signal's variance explained by the different human operator responses was calculated for each participant and is shown in Fig. 10. While the modeled contribution of the crossfeed response $\sigma_{u_c}^2$ to the total operator input σ_u^2 is seen to be relatively minor compared to the visual $\sigma_{u_e}^2$ and vestibular $\sigma_{u_m}^2$ contributions, it still can be quite significant with values up to 20-30% for the roll axis. While still preliminary results, this further underlines the importance of including crossfeed in dual-axis human operator models.

5. DISCUSSION

A human-in-the-loop experiment was performed in a moving-base simulator to investigate the presence of crossfeed in dual-axis manual control. Data was collected from twelve participants performing a compensatory roll and pitch tracking task with fully independent target and disturbance forcing functions in each controlled axis. In addition to the dual-axis condition, reference measurements of the corresponding single-axis pitch and roll tracking behavior were collected for direct comparison.

This study's novel use of independent forcing function signals in the roll and pitch axes facilitated the objective detection of crossfeed, due to the detected presence of consistent off-axis forcing function components in the error and control signals in both primary axes. Furthermore, it allowed for the unique identification of a frequency response estimate of the crossfeed dynamics, in parallel to identifying the operator visual and motion response dynamics. Analysis of identified crossfeed dynamics, together with polar plot analysis of operators' roll and pitch control inputs in the single-axis tasks, suggests the measured crossfeed has a strong motoric component, resulting from operators' apparent inability to give purely single-axis inputs with a dual-axis manipulator. While the spread over different individuals seems appreciable, preliminary human operator modeling results including crossfeed show that the crossfeed contributes up to 20% of the total human control response, thereby suggesting crossfeed is a key attribute of human multi-axis control.

Due to their reliance on frequency-domain analysis, the methods applied in the current paper for crossfeed detection and identification are only valid for linear time-invariant crossfeed effects. While a number of previous investigations also report linear time-invariant crossfeed (Todosiev, 1967; Van Lunteren, 1979), the additional presence of time-varying or nonlinear task interference effects – e.g., resulting from intermittent axis-switching – require further investigation and the development of more sophisticated analysis techniques. Furthermore, our conclusion that the crossfeed measured in our task seems to be predominantly motoric – i.e., stemming from an unintended motoric coupling to the off-axis – does not imply that further crossfeed contributions (e.g., perceptual crossfeed (Levison et al., 1971)) may not be present in human operators as well. Overall, we feel that significant further research is required before the nature of crossfeed in human multi-axis control is satisfactorily understood.

Finally, our experiment results clearly confirm the finding reported in earlier experiments (Mitchell et al., 1990; Zaal and Pool, 2014) that human operators tend to show markedly worse performance in the roll axis in dual-axis roll and pitch control tasks, even for identical task settings. Factors contributing to this effect are a likely prioritization of pitch control by operators (point of emphasis during pilot training), as well as the fact that, due to the nature of the type of the display used, roll errors tend to be less clearly perceivable than pitch errors. When modeling human multi-axis control, for instance for predicting human-in-the-loop performance, awareness of such (voluntary or involuntary) emphasis on one task dimension is another factor that is important to account for.

6. CONCLUSIONS

In this paper, human manual control in dual-axis control tasks with motion feedback has been investigated, with an explicit focus on crossfeed between controlled axes. Overall, our experimental results are consistent with earlier findings and show a clear degradation in task performance and increased remnant in dual-axis tracking, compared to single-axis measurements. Furthermore, measured tracking error and control signal variances – obtained from a dual-axis compensatory tracking task with two independent forcing functions in both axes – show distinct contributions of the off-axis forcing signals, thereby proving the presence of crossfeed. Identified crossfeed responses were found to account for up to 20% of modeled human operator control signals, thereby suggesting the importance of accounting for crossfeed in the analysis and modeling of human multi-axis control.

REFERENCES

Bekey, G., Meissinger, H., and Rose, R. (1965). Mathematical models of human opertors in simple two-axis manual control systems. *IEEE Transactions on Human Factors in Electronics*, HFE-6, 42–52.

Bergeron, H.P., Adams, J.J., and Hurt, G.J. (1971). The Effects of Motion Cues and Motion Scaling on One and Two-Axis Compensatory Control Tasks. Technical Report TN D-6110, NASA Langley Research Center.

Hess, R.A. (2015). Modeling Human Pilot Adaptation to Flight Control Anomalies and Changing Task Demands. *Journal of Guidance, Control, and Dynamics*. Online preprint available.

Jex, H.R., Magdaleno, R.E., and Junker, A.M. (1978). Roll Tracking Effects of G-vector Tilt and Various Types of Motion Washout. In *Proceedings of the Fourteenth Annual Conference on Manual Control*, 463–502.

Levison, W.H., Elkind, J.I., and Ward, J.L. (1971). Studies of Multivariable Manual Control Systems: A Model for Task Interference. Technical Report NASA CR 1746, National Aeronautics and Space Administration.

Mitchell, D.G., Aponso, B.L., and Hoh, R.H. (1990). Minimum Flying Qualities, Volume I: Piloted Simulation Evaluation of in Multiple Axis Flying Qualities. Technical Report WRDC-TR-89-3125, Flight Dynamics Laboratory, Wright-Patterson AFB (OH).

Pool, D.M., Zaal, P.M.T., Damveld, H.J., Van Paassen, M.M., and Mulder, M. (2010). A Cybernetic Approach to Assess Flight Simulator Motion Fidelity. In *Proceedings of the 11th IFAC/IFIP/IFORS/IEA Symposium on Analysis, Design, and Evaluation of Human-Machine Systems, Valenciennes, France*.

Stapleford, R.L., McRuer, D.T., and Magdaleno, R.E. (1967). Pilot Describing Function Measurements in a Multiloop Task. *IEEE Transactions on Human Factors in Electronics*, 8(2), 113–125.

Todosiev, E. (1967). Human Performance in a Cross-Coupled Tracking System. *IEEE Transactions on Human Factors in Electronics*, HFE-8(3).

Van Lunteren, A. (1979). *Identification of Human Operator Describing Function Models with One or Two inputs in Closed Loop Systems*. Ph.D. thesis, Delft University of Technology, Faculty of Mechanical Engineering.

Van Paassen, M.M. and Mulder, M. (1998). Identification of Human Operator Control Behaviour in Multiple-Loop Tracking Tasks. In *Proceedings of the 7th IFAC/IFIP/IFORS/IEA Symposium on Analysis, Design and Evaluation of Man-Machine Systems, Kyoto Japan*.

Zaal, P.M.T. and Pool, D.M. (2014). Multimodal Pilot Behavior in Multi-Axis Tracking Tasks with Time-Varying Motion Cueing Gains. *AIAA Modeling and Simulation Technologies Conference and Exhibit*.